Structure formation from mesoscopic soft particles

A. Fernández-Nieves,[1] J. S. van Duijneveldt,[2] A. Fernández-Barbero,[1] B. Vincent,[2] and F. J. de las Nieves[1,*]
[1]*Group of Complex Fluids Physics, Department of Applied Physics, University of Almería, 04120 Almería, Spain*
[2]*School of Chemistry, University of Bristol, Cantock's Close, Bristol BS8 1TS, United Kingdom*
(Received 10 April 2001; published 22 October 2001)

In this work, the aggregation of mesoscopic gel particles (soft colloids) has been experimentally investigated. The interaction between particles was controlled through the addition of salt, above the critical coagulation concentration, resulting in aggregation with finite bond energies. Attention has been paid to the structure of the clusters formed in the process as well as to the aggregation kinetics. The results indicate that the clusters are fractal and the kinetics of aggregation can be described through the dynamic scaling solution of the Smoluchowski equation. As the energy minimum increases in depth the resultant clusters pass from a very compact structure to typical diffusion-limited cluster aggregation (DLCA) fractal dimension values. In addition, the kinetics of growth change from those observed in reaction controlled aggregation to DLCA. These results can be explained within the framework of a reversible growth model, arising from the fact that aggregation takes place in an energy minimum of restricted depth. Moreover, they show that structure and kinetics decouple for such a soft sphere system, in contrast to what is encountered for DLCA and reaction-limited processes. Finally, an unexpected return to a reaction controlled aggregation kinetics was observed for sufficiently deep energy minima, which could be due to the polymerlike particularities of the soft particles considered in this work.

DOI: 10.1103/PhysRevE.64.051603 PACS number(s): 64.60.Qb

I. INTRODUCTION

Colloidal dispersions mimic almost all phases of condensed matter and serve as excellent model systems. Therefore, studies of *model* colloids under equilibrium and nonequilibrium conditions have helped to provide new insights into phase transitions in atomic systems [1]. Aggregation of particles in colloidal suspensions is an important example of a nonequilibrium process. Conceptually, one starts with a fluidlike system of monomers diffusing by Brownian motion, which due to some sort of attractive interaction aggregate into clusters. These clusters generally have a fractal structure [2] and show a dynamic scaling behavior similar to that observed in systems undergoing spinodal decomposition [3].

In the last decade, both theory and experiments have shown a universal behavior, independent of the particle nature, when the aggregation of clusters is diffusion-limited (DLCA) or reaction-limited (RLCA) [4]. DLCA occurs when every collision between clusters results in the formation of an irreversible bond. This regime gives rise to the formation of branched clusters, with a typical fractal dimension of 1.7–1.8. RLCA occurs when a small fraction of collisions leads to cluster formation. In this case, the aggregates are more compact than those formed in a DLCA process, with a fractal dimension of around 2.1. Moreover, a linear increase of the mean cluster mass with time is characteristic of processes dominated by diffusion, while in the presence of a repulsive energy barrier the mean cluster mass increases with time, as a power law with an exponent larger than one. DLCA and RLCA are limited to certain ideal conditions. In particular, the aggregation must occur in an energy minimum that guarantees the irreversibility of the process. For intermediate aggregation modes, a continuous variation between these two limiting cases is usually found [5].

In addition, the formation of more compact structures than expected for RLCA processes has been encountered and explained in terms of cluster restructuring [6,7] or reaction reversibility [8,9]. In this case, the contacts between particles are considered to be reversible so that they can loosen and reform repeatedly after collision. This reversible mode of aggregation is related to the finite depth of the energy well that holds the particles together. In real industrial systems reversibility is probably the norm rather than the exception. However, very few experimental studies on the growth kinetics and cluster structure are available for these situations, principally due to the difficulties in finding an adequate model system with which controlled flocculation can be achieved.

In this paper, we study the aggregation of dilute, mesoscopic soft spheres (microgel particles). In particular, we have studied the structure of the aggregates formed under high salt conditions (far above the critical coagulation concentration of the colloidal system). The clusters present a more compact structure than expected for DLCA, which may be related to the soft character of these microgel particles, that are able to swell or deswell, depending on the environmental conditions. This feature not only modifies the monomer particle structure and overall size, but also gives rise to the appearance of new contributions to the total interaction potential between particles. If osmotic and elastic effects due to surface interpenetration are taken into account, a finite energy minimum where aggregation may take place develops.

In addition, we have followed the mean cluster size as a function of time. Surprisingly, the short-range interactions appearing as a consequence of the periphery interpenetration

*Author to whom correspondence should be addressed. Email address: fjnieves@ual.es

of the microgel particles also shows up in the growth kinetics. At short times, the process is slower than DLCA, while for long times the cluster size increases with time through a power law characterized by a kinetic exponent greater than one. This behavior is typical of an RLCA process, even though the soft microgel particles do not interact through a long range repulsive interaction that may modify the particles' trajectories. Phase contrast optical microscopy was used for direct observations of some unexpected results, confirming the anomalies encountered by light scattering. Finally, we would like to stress that the structure factor shows dynamic scaling, regardless of the particular form of the kinetics of aggregation.

The outline of the paper is as follows. The first section is a brief theoretical background dealing with the structure factor in aggregating systems. The experimental determination of the cluster fractal dimension and kinetic exponent will be presented within this section. Then, the experimental system and its basic characterization is described, together with the methods. The next section contains the results: cluster structure and kinetics of growth. Finally, these results are interpreted in terms of a reversible growth model.

II. THEORETICAL BACKGROUND

It is well known that colloidal clusters exhibit a fractal morphology, characterized by a fractal dimension d_f. Such structures are formed by a number of particles N that is related to the cluster radius of gyration R through the relation, $N=(R/a)^{d_f}$, where a is the monomer radius. This property manifests in the pair correlation function that scales as [2]

$$g(r)\sim r^{d_f-d}, \tag{1}$$

for an aggregate in a d-dimensional space. In this expression, $d_f<d$ and thus $g(r)\to 0$ as $r\to\infty$, expressing the decay of the local density as the cluster size increases. In experimental scattering studies the function $g(r)$ can be derived by taking the Fourier transform of the structure factor, which is the measurable quantity under the appropriate conditions [10].

Let us consider a colloidal suspension formed by N_m monomer particles. The total structure factor for such a system at a scattering vector $q=4\pi/\lambda \sin(\theta/2)$, with λ the light wavelength in the solvent and θ the scattering angle, is given by

$$S(q)=\sum_{a}^{N_m}\sum_{b}^{N_m} \exp[i\vec{q}\cdot(\vec{r}_a-\vec{r}_b)], \tag{2}$$

where $\vec{r}_a$ is the position of the ath monomer. As can be inferred from this expression, the structure factor contains information concerning the correlations between all particles. If $\vec{r}_a$ is expressed in terms of the center of mass position of the αth cluster $\vec{r}_\alpha$, and of the position of the monomer in the cluster relative to this center of mass, $\vec{r}_i:\vec{r}_a=\vec{r}_\alpha+\vec{r}_i$, equation (2) becomes

$$S(q)=\sum_{\alpha}^{N_c}\sum_{\beta}^{N_c}\sum_{i}^{N}\sum_{j}^{N} \exp[i\vec{q}\cdot(\vec{r}_\alpha-\vec{r}_\beta+\vec{r}_i-\vec{r}_j)] \tag{3}$$

with N_c and N being the number of clusters and particles per cluster, respectively. This expression allows factorization for reasonably monodisperse clusters. Hence

$$S(q)=\sum_{\alpha}^{N_c}\sum_{\beta}^{N_c} \exp[i\vec{q}\cdot(\vec{r}_\alpha-\vec{r}_\beta)]\sum_{i}^{N}\sum_{j}^{N} \exp[i\vec{q}\cdot(\vec{r}_i-\vec{r}_j)], \tag{4}$$

which can be rewritten as

$$S(q)=S_{cc}(q)S_{sc}(q) \tag{5}$$

after defining the cluster-cluster (S_{cc}) and single-cluster (S_{sc}) structure factors. For polydisperse aggregates equation (5) is inexact but constitutes a good approximation [11]. For dilute systems the length scale involved in the cluster-cluster structure factor is too large to be observable in a scattering experiment. As a consequence S_{cc} is constant and $S(q)\sim S_{sc}(q)$. The scale invariance of the fractal clusters ensures that the single cluster structure factor is only a function of the product qR. The relevant information on $S_{sc}(qR)$ is contained in its limiting behavior

$$S_{sc}(q)=\begin{cases}\sim N^2 & qR\ll 1\\ \sim N^2(qR)^{-d_f} & qR\gg 1.\end{cases} \tag{6}$$

Mass conservation during aggregation implies a constant number of monomers in the complete system, $N_m=N_cN$. This consideration implicitly assumes that the system does not gel, i.e., an infinite cluster is formed at infinite time. This is the situation for the dilute aggregating suspensions considered in this work.

In a static light scattering (SLS) experiment, the measurable quantity is the mean scattered intensity I that depends not only on the structure factor but also on the monomer particle form factor $P(q)$. For dilute dispersions,

$$I(q)\sim P(q)S_{sc}(q). \tag{7}$$

The form factor contains information about the interference of light coming from different volume elements within a single particle. For clusters formed by small particles and in the visible light q range, $I(q)\sim S_{sc}(q)$ since the form factor is approximately q independent [12]. As a consequence, the asymptotic behavior of the $I(q)$ curves for $qR\gg 1$, allows determination of the cluster fractal dimension.

An important property of the scattered intensity that can also be used for measuring d_f is that it exhibits dynamic scaling, for sufficiently late aggregation stages, according to

$$I(q,t)\sim q_o^{-d_f}F\left(\frac{q}{q_o}\right), \tag{8}$$

where F is a time-independent scaling function and q_o the scattering vector associated with the characteristic length scale of the system, which contains the time dependence. Remarkably, Eq. (8) is identical in form to the structure factor measured for fluids undergoing spinodal decomposition.

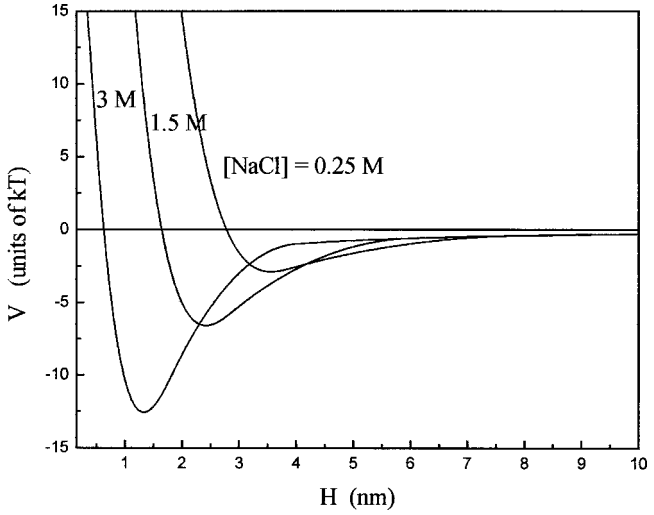

FIG. 1. Interaction potential curves between soft colloidal particles, illustrating the presence of a secondary minimum caused by competing osmotic and elastic interactions (taken from Ref. [24]). The increase in salt concentration results in an increase of the minimum depth. $H=r-d$, with r being the distance between the center of two colloidal particles.

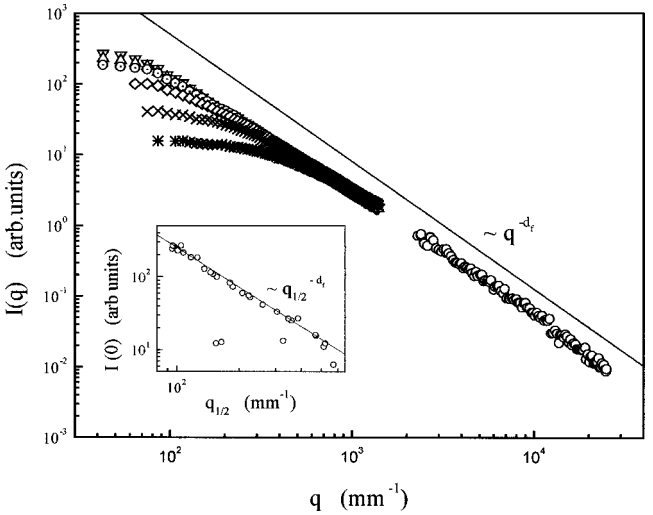

FIG. 2. Intensity vs scattering vector, at different aggregation times. Small-angle light scattering results: *: 10 200 s; × 21 000 s, ◇ 30 000 s, ⊙ 40 800 s, △ 46 200 s, ▽ 53 400 s. Malvern 4700 equipment: ○. In the inset, $I(0)\sim\langle N\rangle$ vs $q_{1/2}\sim R^{-1}$ is plotted. Both figures correspond to $[\mathrm{NaCl}]=3M$, for which $d_f\sim 1.80$.

Moreover, similar structure factors have been observed for other nonequilibrium systems [13]. For the particular case of aggregating particles, this dynamic scaling has been amply studied for highly concentrated suspensions [3,14], even though its physical interpretation still remains unclear in view of the different length scales involved in the problem [11,15]. However, for the dilute case there is only one length scale present in the system, i.e., the cluster size. Thus, whereas the remarkable discovery was that dense aggregating systems exhibit scaling, we see that Eq. (8) strictly applies to the dilute situation.

Finally, we will comment on the growth kinetics. Dynamic light scattering (DLS) is a suitable technique for obtaining details concerning the kinetics of aggregation processes. In particular, information can be extracted from the time evolution of the mean number of particles per cluster, which evolves with time as a power law for advanced aggregation stages [5],

$$\langle N\rangle\sim t^{z}. \tag{9}$$

The kinetic exponent z, contains information on the aggregation mechanism. This growth law exponent is not a universal quantity and depends strongly on the details of the aggregation process [16]. For DLCA processes, $z=1$. When $z>1$ the union of large aggregates dominates and the mean cluster mass increases faster than under diffusion conditions, as for RLCA processes. This lack of universality in the kinetics of growth of an aggregating system is in contrast to the growth law of systems undergoing spinodal decomposition. In the latter case, it is well established that the growth law is given by the Lifshitz-Slyozov law: $\langle N\rangle\sim t$ [17]. The multiple behavior encountered for aggregating colloids, demands a close look at the kinetics of growth. In this paper, the fact that the particles are soft will yield interesting growth laws, which are ascribed by us to be caused by a short-range interaction between particles that arises from surface interpenetration.

III. EXPERIMENTAL DETAILS

A. Experimental system

Mesoscopic gel particles were employed as soft spheres. The synthesis of the system is described elsewhere [19]. The spherical and monodisperse gel particles are based on poly(2-vinylpyridine) (2VP), crosslinked with divinylbenzene (0.25% by weight). The initiator used in the synthesis was 2,2′-azobis(2-amidinopropane) dihydrochloride (V50, Wako).

Two types of chemical groups are able to confer charge to the colloidal particles: (i) amidinium groups arising from the initiator, located essentially at the periphery of the particles, and (ii) the constituent monomer 2VP, located within the particles. In this work, deswollen particles are employed,

TABLE I. Cluster fractal dimension for different salt concentrations. d_f are obtained as indicated by using the Malvern 4700 equipment (second column) and the small-angle light scattering setup (third and fourth columns).

[NaCl] (M)	d_f (I vs q)	d_f [$I(0)$ vs $q_{1/2}$]	d_f (Dynamic scaling)
4	1.793±0.012	1.85±0.08	1.70±0.03
3	1.837±0.014	1.79±0.03	1.70±0.03
2	1.779±0.019	1.85±0.07	1.77±0.03
1.5	1.930±0.023	1.95±0.06	1.95±0.03
1	2.35±0.07	2.35±0.15	2.35±0.03
0.5	2.45±0.06		
0.25	2.45±0.05	2.45±0.16	2.46±0.03

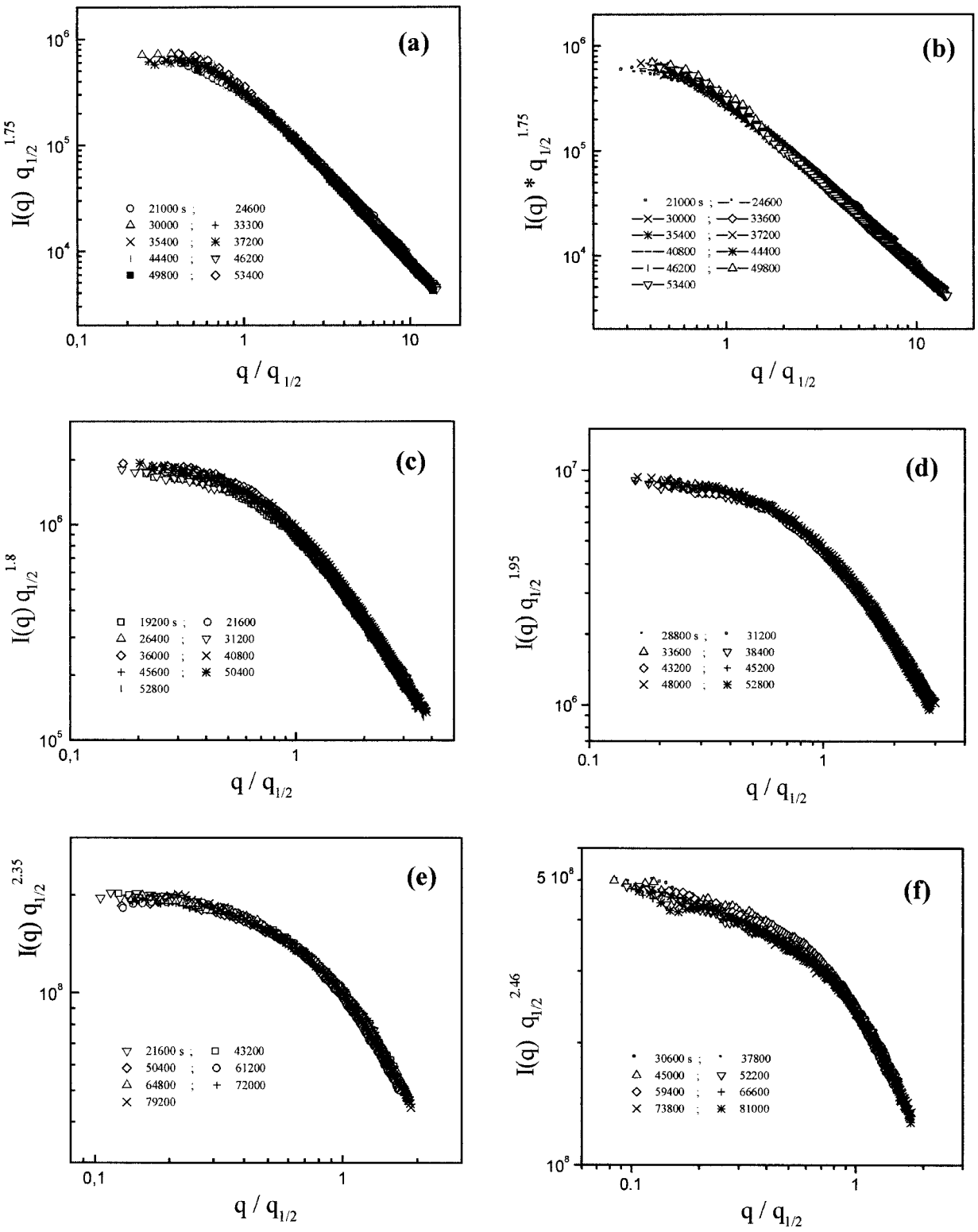

FIG. 3. Dynamic scaling of the scattered intensity for all salt concentrations. Notice the d_f variations for scaling to be achieved. (a) $4M$, (b) $3M$, (c) $2M$, (d) $1.5M$, (e) $1M$, (f) $0.25M$.

with charge only at their surface. Dynamic light scattering was employed for obtaining the mean particle hydrodynamic diameter, yielding $d=(230\pm6)$ nm [20]. The positive sign of the particles was confirmed with the aid of electrophoresis [21].

The system aggregation was induced by addition of salt. The critical coagulation concentration (ccc) was found to be around 30 mM (for NaCl as background electrolyte). Above this ionic concentration, the electrostatic interactions responsible for the colloidal stability are screened out, giving rise to

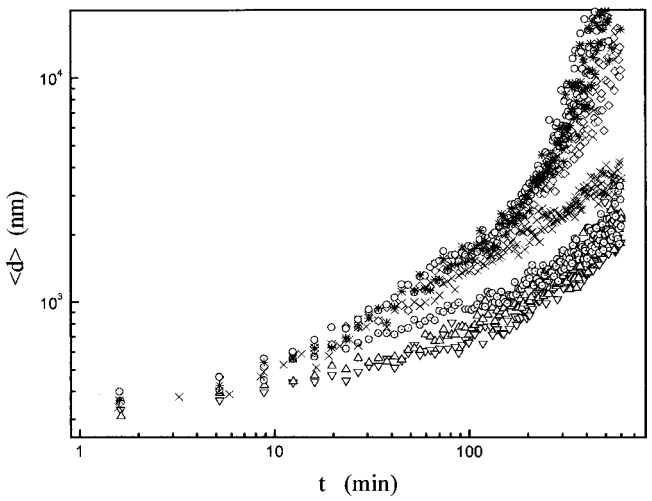

FIG. 4. Mean hydrodynamic diameter as a function of time, for all studied salt concentrations. [NaCl]$=0.25M$ ($\triangledown$), $0.25M$ ($\triangle$), $1M$ ($\odot$), $1.5M$ ($\times$), $2M$ ($\diamond$), $3M$ ($*$), $4M$ ($\bigcirc$).

aggregation [22]. All experiments will be performed far above the ccc.

In addition to destabilizing the system, the addition of salt modifies the polymer-solvent interaction. In particular, it reduces the polymer solvency by favoring the polymer-polymer contacts compared to the polymer-solvent ones [23]. In other words, the addition of salt implies an increase in the polymer Flory χ parameter, which is ~ 0.6 for low salt concentrations [20]. As a result of this effect, the particle size decreases further reducing the particle *softness*, i.e., reducing the interpenetration capacity of the gel particles upon contact.

This salt-induced particle deswelling slightly modifies the microgel particle Hamaker constant, that changes from 6.0×10^{-20} J at $\sim 0.25M$ to 6.6×10^{-20} J at $\sim 3M$, thus leaving the attractive interaction potential almost unaltered [24]. In contrast, it modifies the osmotic and elastic short-range interactions, that are attractive (recall that $\chi > 0.5$) and repulsive, respectively, by diminishing the depth of surface interpenetration and increasing the polymer segment concentration in the overlap zone. These effects, which directly arise from the soft character of the particles, yield a secondary minimum in the interaction potential whose depth increases from $\sim 2.5kT$ at $0.25M$, to $\sim 12.5kT$ at $3M$ (Fig. 1) [24]. Aggregation of the considered experimental system thus occurs in an energy minimum of restricted depth.

B. Instrumental details and experimental conditions

Experiments were performed using two sets of equipment. One was a slightly modified Malvern Instruments 4700 System (UK), working with a 632.8 nm wavelength He-Ne laser. The q range is bound from 2300 to 26 000 mm^{-1}, corresponding to scattering angles between 10° and 150°, respectively. Once the final structure of the clusters was totally established, the mean intensity showed an asymptotic time-independent behavior, as predicted theoretically, from which the fractal dimension was determined.

This apparatus also allows the cluster mean hydrodynamic diameter to be measured using DLS. Intensity autocorrelation functions were determined at different times during aggregation. The scattering angle was set to 70°. The data analysis, based on cumulants, was performed using home-written computer programs.

The second apparatus employed in this work was a small-angle light scattering setup, constructed to be virtually identical to the apparatus described in [25]. It consists of a 5 mW randomly polarized He-Ne laser working at a wavelength of 632.8 nm. The beam was spatially filtered (Melles Griot) to guarantee a Gaussian intensity distribution. After passing the sample, the beam was focused onto a distant projection screen. The light scattering pattern at this screen was not disturbed by the primary laser beam that passed through a hole in the screen and was recorded by a Peltier cooled CCD camera (Lynxx2, SpectraSource) with a resolution of 165×192 pixels. The exposure time was 100 ms and adjustment of the camera diaphragm prevented overflow. Scattering angles were calibrated by imaging light diffracted by a grating. The accessible scattering angles correspond to scattering vectors within the range [50,1500] mm^{-1}. The two-dimensional images recorded by the camera were radially averaged, resulting in arrays of intensity versus scattering vector [26]. During an experiment a series of images was collected and the sample transmission was measured with a photodiode. The time series was corrected for dark current and stray-light contributions by subtracting a prior blank measurement. Intensities were normalized for the increasing turbidity by dividing by transmission [25,27].

Optical microscopy experiments were carried out using an optical transmission phase contrast Nikon microscope (Japan). Pictures were captured directly by a CCD-camera (Intellicam, USA) and no image treatment was applied.

All measurements were carried out under very dilute conditions, with the particle concentrations being equal to 2×10^9 cm^{-3} for SLS experiments and 5×10^9 cm^{-3} for DLS and optical microscopy. The medium pH was in the range 5.5–6 for all the experiments, whilst the ionic concentration was adjusted with NaCl. The temperature was constant and equal to (25.0 ± 0.1) °C.

IV. EXPERIMENTAL RESULTS

A. Cluster morphology and dynamic scaling

The fractal dimension of clusters formed by the aggregation of soft particles was obtained using Eqs. (6) and (8), at salt concentrations far above 30 mM. The $I(q)$ curve for the case [NaCl]$=3M$ is shown in Fig. 2. Similar curves were obtained at any other salt concentrations.

At a given aggregation stage, the $I(q)$ curves show a q-independent Rayleigh regime at low scattering vectors. At higher q, a bend in the curves occurs when the characteristic length scale of the scattering becomes comparable to the cluster size. The precise q value at which this bend takes place, q_0, allows the mean cluster size to be determined. At increasing scattering vectors, the asymptotic behavior of the structure factor is reached, allowing the determination of d_f (see Fig. 2).

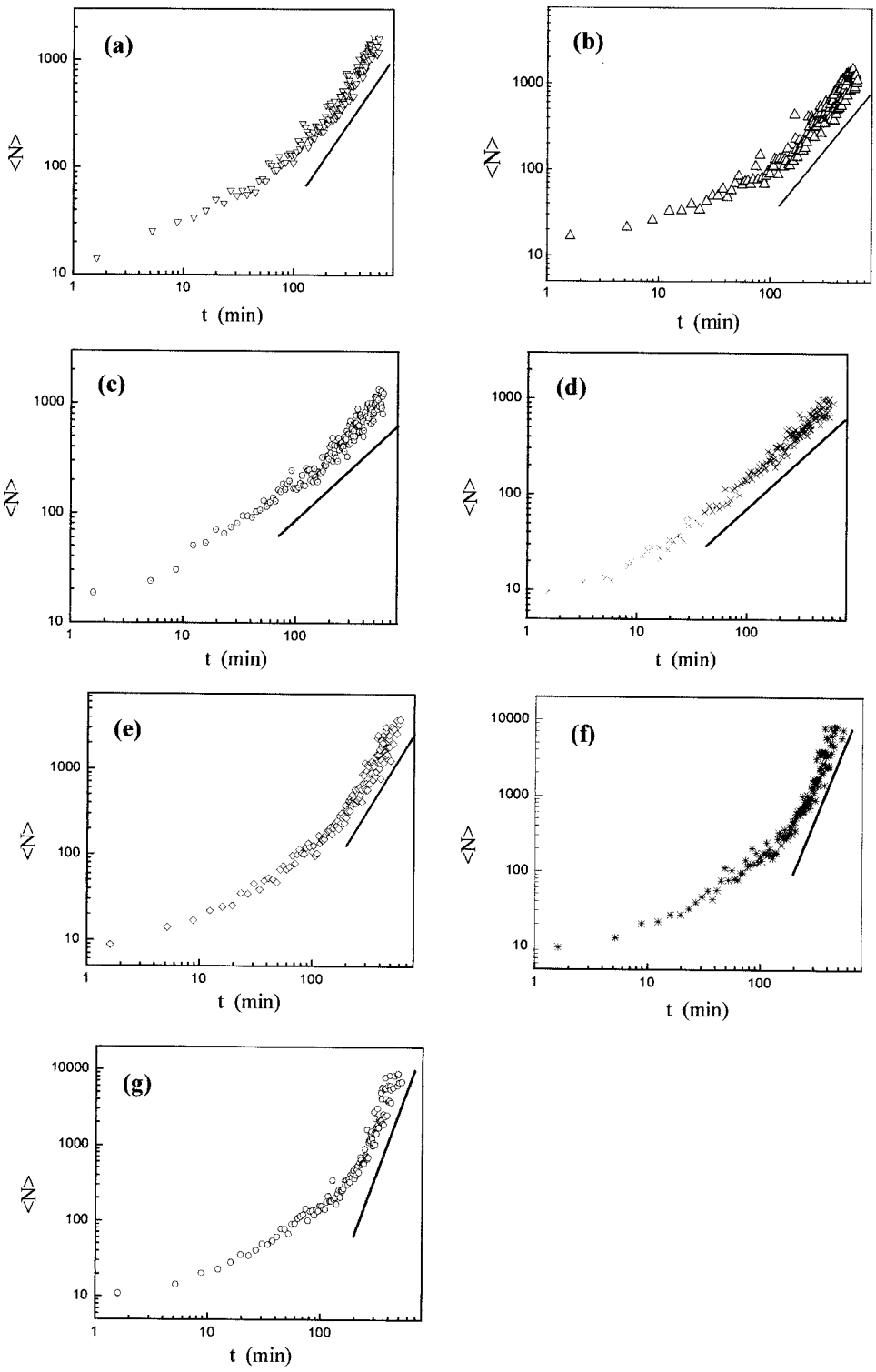

FIG. 5. Mean number of particles per cluster as a function of time. The asymptotic power law from which z is obtained is shown. (a) $0.25M$, (b) $0.5M$, (c) $1M$, (d) $1.5M$, (e) $2M$, (f) $3M$, (g) $4M$.

Further analysis of the $I(q)$ curves allows $I(0)$ to be obtained by extrapolation of the low-q-region scattered intensities and of $q_{1/2}$, the latter being the scattering vector for which the scattered intensity $I(0)$ decays to half its value. The time dependence of $q_{1/2}$ mimics that of q_0, since both scattering vectors reflect the cluster size growth as aggregation proceeds. We prefer to work with $q_{1/2}$ instead of q_0, since this scattering vector can be determined more confidently [28]. A plot of $I(0)$ vs $q_{1/2}$ permits the evaluation of d_f, since the scattered intensity $I(0)$ is proportional to the mean number of particles within an aggregate [29] and $q_{1/2} \sim R^{-1}$ (see inset of Fig. 2).

Results for all the salt concentrations studied are presented in Table I. As can be seen, the fractal dimensions increase from $\sim$1.7–1.8 to $\sim$2.45, as the ionic concentration decreases from $4M$ to $0.25M$, respectively. It is interesting to note that d_f changes with salt concentration, since at the NaCl concentrations studied, the electrostatic interaction is

TABLE II. Kinetic exponent for different salt concentrations.

[NaCl] (M)	z
4	3.80 ± 0.06
3	3.40 ± 0.06
2	2.25 ± 0.05
1.5	1.00 ± 0.02
1	1.00 ± 0.04
0.5	1.46 ± 0.05
0.25	1.60 ± 0.06

totally screened out. The increase in χ as the medium ionic concentration is increased modifies the interaction potential between particles, thus affecting the cluster structure, which departs from expected DLCA behaviors. Notice that d_f has been obtained by two independent ways and using two different experimental setups, covering almost three decades in q.

To further corroborate the estimates of the fractal dimension we explored the dynamic scaling established by Eq. (8) which should be strictly valid under dilute conditions, since, in this situation, the system is controlled by a single length scale corresponding to the cluster size. Figure 3 shows the results. It can be observed that the scaling law works very well, independent of the particular aggregation mechanism that leads to different cluster fractal dimensions. Pictorially, this scaling implies that the system configuration at an earlier time, after homogeneous magnification at a suitable scale, should be statistically indistinguishable from a configuration at a later time. A common feature for all the curves is that, during their growing process, the clusters are randomly positioned in space, with no correlation between them at any time. Finally, it is worth stressing that the fractal dimensions needed for scaling to be achieved agree remarkably with prior determinations (Table I).

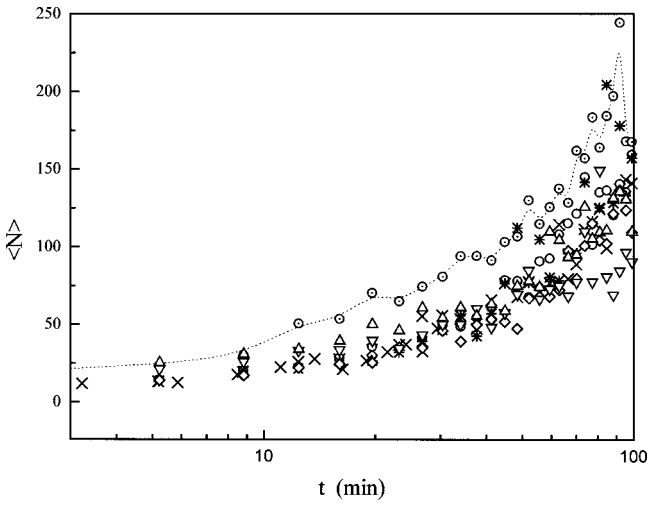

FIG. 6. Mean number of particles per cluster for short times, at different salt concentrations. [NaCl]$=0.25M$ ($\triangledown$), $0.5M$ ($\triangle$), $1M$ ($\odot$), $1.5M$ ($\times$), $2M$ ($\diamond$), $3M$ ($*$), $4M$ ($\bigcirc$).

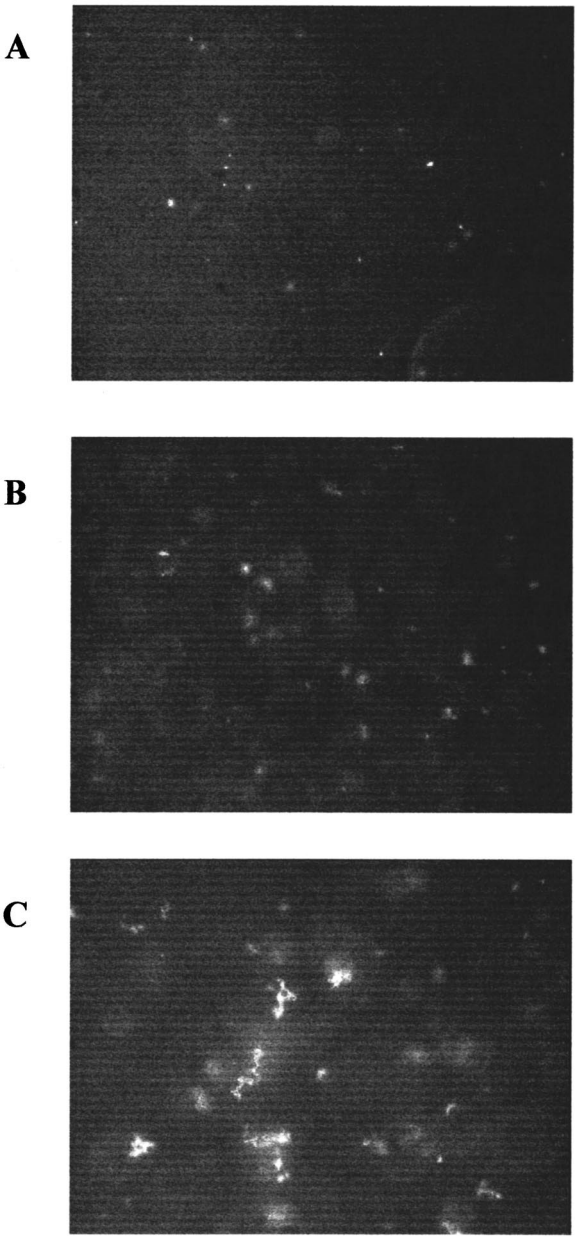

FIG. 7. Optical micrographs of aggregated samples by transmission phase contrast optical microscopy at 7 h from the onset of aggregation. (a) $1M$, (b) $2M$, (c) $3M$.

B. Kinetics of aggregation

Figure 4 shows the time evolution of the mean cluster hydrodynamic diameter for all the salt concentrations studied. The cluster size increases with time, as expected, but in different ways, depending on the experimental conditions, even though the ccc is considerably surpassed. The mean aggregate size contains both information on the reaction kinetics as well as on the cluster structure. For obtaining kinetic information only, one may use the mean number of particles per cluster that can be derived by making use of the previously determined fractal dimensions. Figure 5 shows the results. All the curves exhibit a power law in time, at sufficiently large times. This means that the dynamic scaling

solution for the Smoluchowski equation is suitable for describing the aggregation processes studied here.

From the asymptotic behavior of the $\langle N\rangle(t)$ curves, the kinetic exponent can be obtained [Eq. (9)]. The results are presented in Table II. As can be seen, z changes with salt concentration, indicating that the interparticle interaction is being altered. For $[\mathrm{NaCl}]=1$, $1.5M$, $z=1$, corresponding to diffusion controlled kinetics. Above and below those ionic concentrations, $z>1$, as for reaction controlled aggregation (RCA) processes. In these latter cases, the short time kinetics are slower than DLCA. It is at longer times when $\langle N\rangle$ reaches the asymptotic power law behavior. In order to further analyze the results, we have checked the short time behavior of $\langle N\rangle$ at all salt concentrations (Fig. 6). As can be seen, the aggregation at $[\mathrm{NaCl}]=1M$ is the fastest for t up to $\sim$100 min.

The kinetic results show that, as the salt concentration increases, the aggregation mechanism is analogous to a process controlled by reaction, until a given ionic concentration is reached. Then, the kinetics become diffusion controlled. At even higher salt concentrations the aggregation process becomes again characterized by a kinetic exponent $z>1$. The analogy with RCA not only manifests at long times, but also in the initial stages, where those processes are slower than DLCA. It is worth stressing that all salt concentrations are far above the ccc, thus assuring that the electrostatic interaction between the particles plays no role. Moreover, a similar phenomenology is obtained as for RCA, even though the only possible interactions between particles are very short range.

V. INTERPRETATION OF THE RESULTS: REVERSIBLE GROWTH MODEL

For electrostatically stabilized suspensions, addition of salt above the ccc should, intuitively, leave the aggregation mechanism unchanged. The fractal dimension of aggregates formed under these circumstances should be constant and equal to 1.7–1.8 and the kinetic exponent $z=1$, which are typical values for diffusion controlled aggregation. The growth kinetics and the structure of the clusters formed by the aggregation of mesoscopic gel particles do not show these features, indicating that the aggregation mechanism is being altered. The explanation for this unexpected behavior has its origin in the soft character of the microgel surface, which permits some interpenetration of polymer chains. As a consequence, the total interaction potential between gel-like particles shows a secondary minimum, whose depth is controlled by the salt concentration through modification of the polymer χ parameter (see Fig. 1).

The interpretation of the results is straightforward in terms of the reversible growth model, first introduced by Shih, Aksay, and Kikuchi (SAK) [8]. This is basically a simulation model, built by modifying the classical cluster-cluster aggregation model with a finite interparticle attraction energy, $-V_{\mathrm{min}}$. The aggregation reversibility is attained by introducing a probability for unbinding to occur, $P\sim\exp[-nV_{\mathrm{min}}/(kT)]$, where n is the number of closest neighbors of every single particle. Reducing V_{min} results in increasing the probability for unbinding. In the limit $V_{\mathrm{min}}\rightarrow\infty$, $P\rightarrow 0$ and the predictions of the cluster-cluster aggregation model are recovered. Clearly, local particle structures become substantially more stable as the number of bonded neighbors per particle increases. Therefore, the presence of the finite bond energy encourages compactification of clusters. On the other hand, the finiteness of V_{min} enhances the reversibility of the growth process. As a consequence, the overall growth is slowed down with respect to DLCA, due to thermal annealing of clusters.

The decrease in the fractal dimension with the increase in salt concentration (see Table I) can be understood as an aggregation process taking place in a finite energy minimum, which increases in depth as the ionic concentration is raised. As the minimum becomes deeper, the probability for unbinding decreases and the cluster structure becomes more branched. As the energy minimum depth is reduced, the number of particle neighbors n has to increase in order to reduce the probability for unbinding, thus yielding higher fractal dimensions. The agreement with SAK simulations is more than qualitative: $d_f\sim 2.4-2.5$ are predicted for $V_{\mathrm{min}}/(kT)\sim 2-3$, in total accordance with the experimental results. Moreover, $d_f\sim 1.7-1.8$ is predicted for energy minima above $\sim 9kT$, which is also in agreement with our results.

The observed aggregation kinetics can also be understood within the framework of a reversible growth mechanism. As the salt concentration decreases from $1.5M$, the energy minimum depth decreases, thus enhancing the reversibility of the process. This means that the growth becomes slower than for a DLCA process, as experimentally observed. As the reaction proceeds, aggregation is energetically favored and $z>1$ is obtained. The same situation is encountered for processes in between DLCA and RLCA, even though the physical picture is different. However, the fact that RLCA phenomenology is in many cases computer simulated by introducing a sticking probability S between clusters [18], throws light on this analogy. Introduction of a sticking probability simplifies the experimental reaction limited aggregation, since for this situation the presence of the long-range repulsion modifies the particles' trajectories, while in the simulations the approach of the particles is diffusive and only upon contact a decision is taken on whether the clusters should stick or not. In the spirit of these simulation results, short-range interactions between colloids could dramatically modify the aggregation kinetics, yielding similar results as those reported for RCA processes. The reversibility of aggregation in the current system is related to a sticking probability, $S=1-P$. As [NaCl] decreases below $1.5M$, the probability for unbinding increases (V_{min} decreases) and S decreases, implying an approach to the RLCA phenomenology.

Surprisingly, above $[\mathrm{NaCl}]=1.5M$, the kinetic exponent becomes greater than 1, again at sufficiently long times. In order to further validate this increase in z, transmission phase contrast optical microscopy was used to make direct observations of the aggregates formed at salt concentrations above $1.5M$. Figure 7 shows the optical micrographs corresponding to aggregation at $1M$, $2M$, and $3M$, after 7 h. It is clearly seen that the clusters are bigger, the higher the ionic concen-

tration, in agreement with the prior experimental findings (see Fig. 4) and supporting the measured *z* values. However, we do not have a clear explanation for such unexpected behavior. Polymer relaxation effects in a time scale higher than the Brownian scale could induce variations in the interaction potential that could also be manifested in the aggregation kinetics. If this is the case, then this effect would tend to occur at high salt concentrations, when the polymer concentration in the overlap zone between particles is high enough for the effect to become important. Nevertheless, the encountered behavior has been demonstrated by different studies in this work, demanding further research.

VI. CONCLUSIONS

Structure formation from mesoscopic gel particles (soft colloids) has been experimentally studied using static and dynamic light scattering. The interaction between the particles was controlled through the addition of salt, above the critical coagulation concentration, resulting in aggregation with finite bond energies. The resultant clusters are fractal and the kinetics of aggregation can be described through the dynamic scaling solution of the Smoluchowski equation. As the energy minimum increases in depth, the resultant clusters pass from a very compact structure, characterized by fractal dimensions as high as 2.45, to typical DLCA values. On the other hand, the kinetics of growth change from those observed in reaction controlled aggregation, which are characterized by a kinetic exponent greater than 1, to DLCA. These results can be explained within the framework of a reversible growth model, arising from the fact that aggregation takes place in an energy minimum of finite depth. It is worth stressing that the experimental fractal dimensions are in quantitative agreement with simulations of reversible growth behavior. Moreover, the analogy between the encountered kinetics and those controlled by interparticle repulsive forces is remarkable, since in our case the interaction potential is very short range. The reversible growth behavior, observed experimentally, is analogous to simulations where sticking probabilities are considered. As an overall conclusion, we have encountered that the aggregation of soft gel particles has features that scape from the two universal regimes. In particular, structure and kinetics decouple, in contrast to what is encountered for DLCA and RLCA processes. Finally, for sufficiently deep energy minima, an unexpected return to a reaction controlled aggregation kinetics was observed and corroborated with the aid of phase-contrast optical microscopy. Such strange behavior could be due to the particularities of the soft particles considered in this work and at present time is under investigation.

ACKNOWLEDGMENTS

The financial support under project MAT2001-2767 is greatly acknowledged. A. F.-N expresses his gratitude to the Acción Integrada Hispano-Británica (HB 1998-0225) for granting a one-month stay at the University of Bristol. J.S.v.D wishes to thank the Nuffield Foundation (Ref. NUFNAL) for support.

[1] A. K. Arora and R. Rajagopalan, Curr. Opin. Colloid Interface Sci. **2**, 391 (1997).
[2] T. Vicsek, *Fractal Growth Phenomena* (World Scientific, Singapore, 1992).
[3] M. Carpineti and M. Giglio, Phys. Rev. Lett. **68**, 3327 (1992).
[4] M. Carpineti and M. Giglio, Adv. Colloid Interface Sci. **46**, 73 (1993).
[5] D. Asnaghi, M. Carpineti, M. Giglio, and M. Sozzi, Phys. Rev. A **45**, 1018 (1992).
[6] C. Aubert and D. S. Cannell, Phys. Rev. Lett. **56**, 738 (1986).
[7] M. Tirado-Miranda, A. Schmitt, J. Callejas-Fernández, and A. Fernández-Barbero, Langmuir **15**, 3437 (1999).
[8] W. Y. Shih, I. A. Aksay, and R. Kikuchi, Phys. Rev. A **36**, 5015 (1987); J. Lin, W. Y. Shih, M. Sarikaya, and I. A. Aksay, *ibid.* **41**, 3206 (1990); W. Y. Shih, J. Liu, W. H. Shih, and I. A. Aksay, J. Stat. Phys. **62**, 961 (1991).
[9] M. D. Haw, M. Sievwright, W. C. K. Poon, and P. N. Pusey, Physica A **62**, 1 (1995).
[10] J. K. G. Dhont, *An Introduction to Dynamics of Colloids* (Elsevier, Amsterdam, 1996).
[11] H. Huang, C. Oh, and C. M. Sorensen, Phys. Rev. E **57**, 875 (1998).
[12] M. Y. Lin, H. M. Lindsay, D. A. Weitz, R. C. Ball, R. Klein, and P. Meakin, Phys. Rev. A **41**, 2005 (1990).
[13] J. Marro, J. L. Lebowitz, and M. H. Kalos, Phys. Rev. Lett. **43**, 282 (1979); H. L. Snyder and P. Meakin, J. Chem. Phys. **79**, 5588 (1983).
[14] M. Carpineti and M. Giglio, Phys. Rev. Lett. **70**, 3828 (1993).
[15] M. D. Haw, M. Sievwright, W. C. K. Poon, and P. N. Pusey, Physica A **217**, 231 (1995).
[16] T. Sintes, R. Tóral, and A. Chakrabarti, Phys. Rev. E **50**, R3330 (1994).
[17] I. M. Lifshitz and V. V. Slyozov, J. Phys. Chem. Solids **19**, 35 (1961).
[18] F. Family, P. Meakin, and T. Vicsek, J. Chem. Phys. **83**, 4144 (1985); S. Stoll and E. Pefferkorn, J. Colloid Interface Sci. **160**, 149 (1993); **177**, 192 (1996).
[19] A. Loxley and B. Vincent, Colloid Polym. Sci. **275**, 1108 (1997).
[20] A. Fernández-Nieves, A. Fernández-Barbero, B. Vincent, and F. J. de las Nieves, Macromolecules **33**, 2114 (2000).
[21] A. Fernández-Nieves, A. Fernández-Barbero, and F. J. de las Nieves, Phys. Rev. E **63**, 041404 (2001).
[22] A. Fernández-Nieves, A. Fernández-Barbero, and F. J. de las Nieves, Phys. Rev. E **64**, 032401 (2001).
[23] P. W. Zhu and D. H. Napper, Colloids Surf., A **98**, 106 (1995).
[24] A. Fernández-Nieves, A. Fernández-Barbero, B. Vincent, and F. J. de las Nieves, Langmuir **17**, 1841 (2001).
[25] N. A. M. Verhaegh, J. S. van Duijneveldt, J. K. G. Dhont, and H. N. W. Lekkerkerker, Physica A **230**, 409 (1996).

[26] W. C. K. Poon and M. D. Haw, Adv. Colloid Interface Sci. **73**, 71 (1997).

[27] T. Hashimoto, M. Itakura, and H. Hasegawa, J. Chem. Phys. **85**, 6118 (1986).

[28] K. Schätzel and B. J. Ackerson, Phys. Rev. Lett. **68**, 337 (1992).

[29] M. Carpineti, F. Ferri, M. Giglio, E. Paganini, and U. Perini, Phys. Rev. A **42**, 7347 (1990).